# Regulation of Microtubule-Dependent Protein Transport by the TSC2/Mammalian Target of Rapamycin Pathway

Xiuyun Jiang and Raymond S. Yeung

Department of Surgery, University of Washington, Seattle, Washington

## Abstract

Protein transport plays a critical role in the interaction of the cell with its environment. Recent studies have identified *TSC1* and *TSC2*, two tumor suppressor genes involved in tuberous sclerosis complex, as regulators of the mammalian target of rapamycin (mTOR) pathway. Cells deficient in TSC1 or TSC2 possess high levels of Rheb-GTP resulting in constitutive mTOR activation. We have shown previously that the TSC1/TSC2 complex is involved in post-Golgi transport of VSVG and caveolin-1 in mammalian cells. Here, we show that modulation of mTOR activity affects caveolin-1 localization and that this effect is independent of p70S6K. *Tsc1*- and *Tsc2*-null cells exhibit abnormal caveolin-1 localization that is accompanied by disorganized microtubules in the subcortical region. Analyses of green fluorescent protein-EB1 and tubulin in live mutant cells suggest a failure of the plus-ends to sense cortical signals and to halt microtubule growth. Down-regulation of CLIP-170, a putative mTOR substrate with microtubule-binding properties, rescued the abnormal microtubule arrangement and caveolin-1 localization in *Tsc2*−/− cells. Together, these findings highlight a novel role of the TSC2/mTOR pathway in regulating microtubule-dependent protein transport. (Cancer Res 2006; 66(10): 5258-69)

## Introduction

The phosphatidylinositol 3-kinase (PI3K)/AKT/mammalian target of rapamycin (mTOR) pathway has been implicated in many sporadic human cancers, including prostate, breast, endometrium, glioma, etc. (1). In addition, mTOR activation is a common phenomenon observed in tumors arising from several hereditary syndromes, including Cowden's disease, tuberous sclerosis, Peutz-Jeghers syndrome, and neurofibromatosis 1 (2). The underlying genetic defects of these syndromes involve the *PTEN, TSC1* and *TSC2, LKB1*, and *NF1* tumor suppressor genes, respectively, whose biochemical functions are at least partially linked to the regulation of mTOR activity. The pathologic features of the lesions associated with these tumor-predisposing syndromes illustrate abnormalities in cell growth, proliferation, differentiation, and migration, suggesting a function of mTOR signaling in mediating these biological processes.

Recent investigations of the TSC1/TSC2 tumor suppressor genes have uncovered their connections to the mTOR pathway (reviewed in ref. 3). Serving as a GTPase-activating protein (GAP), the TSC1/TSC2 heterodimer promotes hydrolysis of Rheb-GTP, a member of the Ras superfamily of G proteins, to negatively regulate mTOR (4–8). In turn, the activity of TSC1/TSC2 is controlled by multiple phosphorylation events downstream of kinases, including AKT and AMPK. Growth factors, such as insulin, stimulate PI3K/AKT to inhibit TSC2 (9–11), whereas glucose and ATP prevent AMPK-dependent phosphorylation of TSC2 (12, 13), both of which result in mTOR activation. The latter promotes protein synthesis via p70S6K-mediated ribosomal biogenesis and 4E-BP1-dependent translation of 5′-capped RNAs. This function of mTOR requires the rapamycin-sensitive mTORC1 complex consisting of raptor and mLST8 (also known as GβL) in addition to mTOR (14, 15). Alternatively, mTOR can associate with rictor and mLST8 to form a rapamycin-insensitive mTORC2 complex that regulates AKT activity and the actin cytoskeleton (16, 17). Currently, the biological effects of mTOR on cell morphology and cytoskeletal arrangement remain poorly understood.

The mTOR pathway plays a central role in controlling cell growth and metabolism in response to nutrients, such that the availability of amino acids and glucose modulates mTOR activity (18). There is also evidence that TOR activity could regulate nutrient transport by affecting the distribution of the transporters within the cell. For example, observations from *Saccharomyces cerevisiae* suggest that a component of the TOR complex, LST8, is involved with the late secretory delivery of Gap1p, an amino acid permease, to the membrane (19). The relationship between TOR and protein transport has not been elucidated. In mammalian cells, polycystin-1 is abnormally retained in the Golgi of *Tsc2*−/− cells in which mTOR activity is constitutively activated (20). We subsequently showed that post-Golgi trafficking of VSVG-green fluorescent protein (GFP) and caveolin-1 is under the regulation of TSC2 (21). Consequently, in *Tsc2*−/− cells, these proteins failed to be transported to the plasma membrane and remained in punctate cytoplasmic vesicles. Expression of exogenous Tsc1 and Tsc2 in these mutant cells restored caveolin-1 to the plasma membrane. In this study, we tested the hypothesis that the abnormal protein transport in *Tsc2*−/− cells is due to unregulated mTOR signaling. The results show that caveolin-1 transport is modulated by components of the mTOR pathway, Rheb, mTOR, and mLST8, but not p70S6K. Further, the trafficking defect in *Tsc2*−/− cells is associated with an underlying abnormality in microtubule organization. Down-regulation of CLIP-170, a mTOR substrate that binds microtubules, is sufficient to rescue the cytoskeletal defect and the abnormal caveolin-1 distribution in *Tsc2*−/− cells. These results highlight a novel function of the mTOR pathway in microtubule organization and provide insights into how cells regulate intracellular trafficking in response to environmental signals and nutrients.

## Materials and Methods

**Chemicals, antibodies, and plasmids.** Cell culture reagents, Lipofect-AMINE, and PLUS were purchased from Invitrogen, Inc. (Carlsbad, CA). Acrylamide was obtained from National Diagnostics (Atlanta, GA).

Immobilon-P polyvinylidene difluoride membranes were purchased from Millipore (Bedford, MA). The anti-caveolin-1 [monoclonal antibody (mAb)] and anti-p70S6K (mAb) were from BD Biosciences (San Diego, CA) and anti-caveolin-1 (polyclonal antibody, N-20) antibody was obtained from Santa Cruz Biotechnology (Santa Cruz, CA). The polyclonal anti-c-myc (M5546), monoclonal anti-myc (9E10), anti-mouse α-tubulin (DM1A), and anti-mouse actin antibodies were purchased from Sigma Chemical Co. (St. Louis, MO). Other antibody reagents included polyclonal anti-hemagglutinin (HA) antibody (Covance Research Products, Berkeley, CA), monoclonal anti-HA antibody (Roche Diagnostics, Indianapolis, IN), and phospho-p70S6K (Thr[389]), phospho-S6 (235/236), S6, AKT, and phospho-AKT (Ser[473]) anti-bodies (Cell Signaling, Beverly, MA). Alexa Fluor 488–conjugated anti-mouse and anti-rabbit antibodies and Alexa Fluor 568–conjugated anti-mouse and anti-rabbit antibodies were obtained from Molecular Probes (Eugene, OR). Horseradish peroxidase–conjugated anti-rabbit and anti-mouse antibodies and enhanced chemiluminescence (ECL) reagent were obtained from Amersham Pharmacia Biotech (Piscataway, NJ). The polyclonal anti-CLIP-170 antibody and myc-CLIP-170 plasmid were gifts from S. Zheng (Washington University, St. Louis, MO). Anti-mouse acetylated tubulin antibody was obtained from Sigma. pEGFPN1-EB1 and pEGFP-tubulin plasmids were gifts from L. Wordeman (University of Washington, Seattle, WA). Cy3-luciferase small interfering RNA (siRNA) was purchased from
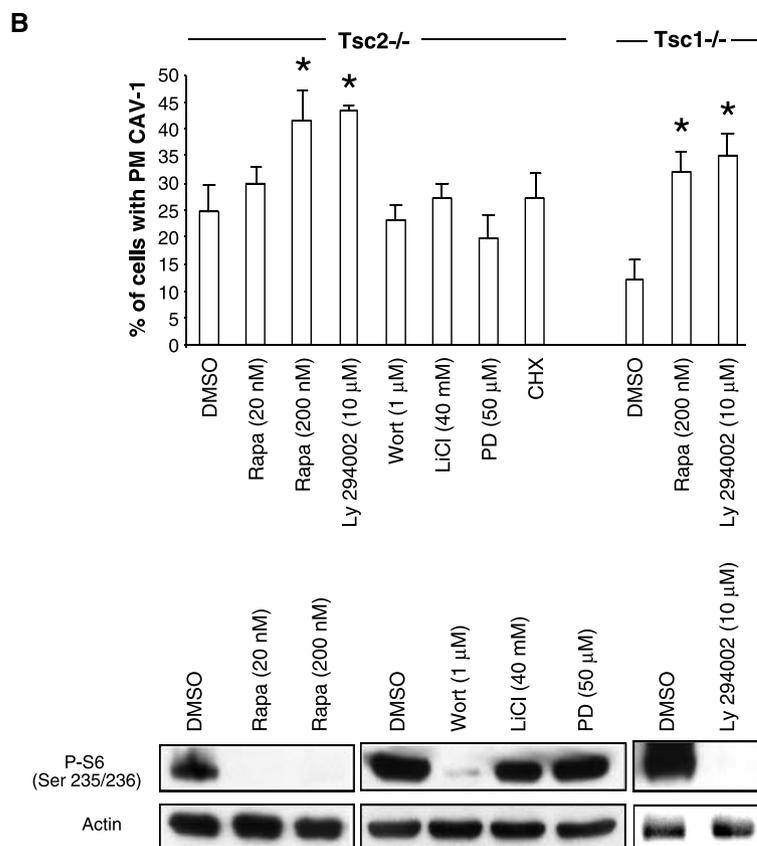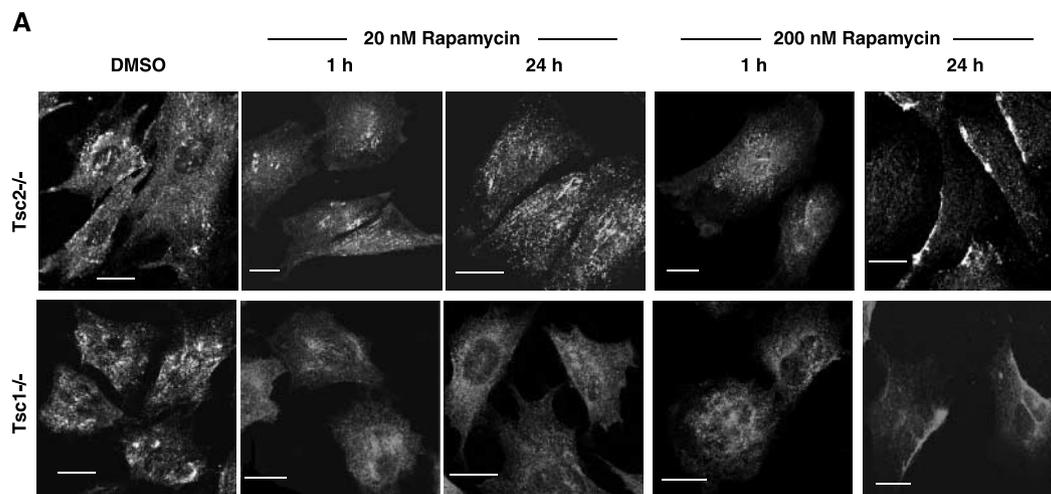


**Figure 1.** Effects of rapamycin on caveolin-1 localization. *A, Tsc2−/−* REFs (EEF-8) and *Tsc1−/−* MEFs were treated with low-dose (20 nmol/L) or high-dose (200 nmol/L) rapamycin or control (DMSO) for 1 or 24 hours. Immunofluorescence analysis was done using antibodies against caveolin-1 and viewed with confocal microscope (Leica). Bar, 20 μm. *B,* proportion of *Tsc2−/−* and *Tsc1−/−* cells with plasma membrane (*PM*) localization of caveolin-1 (*CAV-1*) following treatment with various drugs: 20 and 200 nmol/L rapamycin (*Rapa*), 10 μmol/L LY294002, 1 μmol/L wortmannin (*Wort*), 40 mmol/L lithium chloride (*LiCl*), 50 μmol/L PD98059 (*PD*), and 50 μg/mL cycloheximide (*CHX*). *, $P < 0.05$, compared with DMSO for all other treatments; $P > 0.1$, compared with DMSO. Western blotting of *Tsc2−/−* cell lysates with anti-phospho-S6 and anti-actin antibodies corresponding to the treatments.
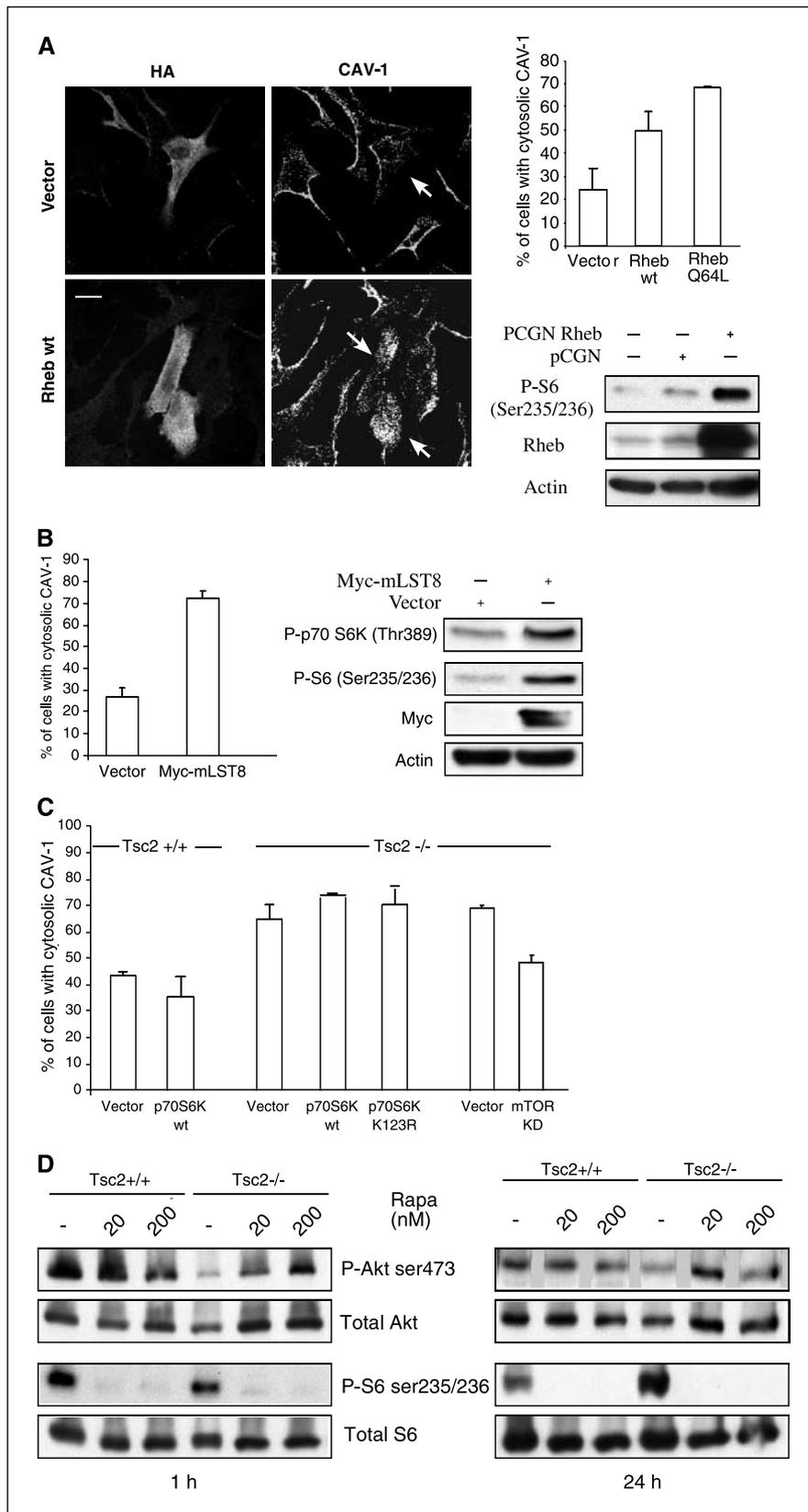
**Figure 2.** Effects of Rheb, mLST8, mTOR, and p70S6K on caveolin-1 distribution. *A, Tsc2+/+* (EEF-4) REFs were transfected with HA-tagged Rheb or empty vector for 48 hours and processed for immunofluorescence using antibodies for HA and caveolin-1. Note that the wild-type (*wt*) cells normally exhibit plasma membrane caveolin-1 localization. *Arrows,* transfected cells. Bar, 20 μm. *Columns,* proportion of transfected cells with predominant cytosolic caveolin-1 distribution tabulated from three independent experiments. Western blot analysis shows the effect of Rheb expression on S6 phosphorylation in *Tsc2+/+* cells. *B,* effects of mLST8 expression on caveolin-1 distribution (*columns*) and mTOR signaling (Western blot) in *Tsc2+/+* cells. *C, Tsc2+/+* and *Tsc2−/−* cells were transfected with wild-type p70S6K, kinase-deficient (K123R) mutant, or kinase-inactive mTOR (S2035T/D2357E); note the resultant caveolin-1 distribution. *D,* effect of rapamycin on AKT activity. *Tsc2+/+* and *Tsc2−/−* cells were starved overnight and stimulated with 10% FBS (30 minutes) followed by rapamycin treatment (0, 20, and 200 nmol/L) for 1 hour (*left*) and 24 hours (*right*). Immunoblot analysis was done using indicated antibodies.

Upstate Biotechnology (Lake Placid, NY) and predesigned rat Cy3-CLIP-170 siRNA (ID no. 54147) was from Ambion, Inc. (Austin, TX). Rapamycin, wortmannin, LY294002, and PD98059 were obtained from Calbiochem (La Jolla, CA). Lithium chloride was purchased from Sigma. HA-tagged Rheb wild-type plasmid and anti-rabbit Rheb 780 antibody were kindly supplied from G. Clark (NIH, Rockville, MD). Myc-tagged Rheb(Q64L) (constitutively active form) plasmid was kindly provided by K-L. Guan (University of Michigan, Ann Arbor, MI). The p70S6K wild-type and p70S6K(K123R)

(inactive KR mutant) plasmids were kindly supplied from D. Templeton (Case Western Reserve University, Cleveland, OH). pCI-myc-human LST8 was kindly supplied from E. Jacinto/M. Hall (University of Basel, Basel, Switzerland; ref. 22). The kinase-inactive mTOR (S2035T/D2357E) construct was a gift from J. Chen (University of Illinois, Urbana, IL; ref. 23).

**Cell culture and transfection.** $Tsc2+/+$ (EEF-4) and $Tsc2-/-$ (EEF-8 and EEF-4A) rat embryonic fibroblasts (REF) and $Tsc1+/+$ and $Tsc1-/-$ mouse embryonic fibroblasts (MEF; gift of David Kwiatkowski, Harvard University, Boston, MA) were grown in DMEM/F-12 or DMEM containing 10% fetal bovine serum (FBS) as described previously (21). Transfections with plasmids or siRNAs (final concentration, 100 nmol/L) were done using LipofectAMINE and PLUS according to the manufacturer's instructions. For FBS starvation, cells or cells 24 hours post-transfection of Rheb or mLST8 were cultured with serum-free DMEM/F-12 for 24 hours. Forty-eight hours post-transfection, cells were harvested for analysis by Western blot or fixed for analysis by indirect immunofluorescence analysis.

**Western blot.** Cells were washed twice with ice-cold PBS and then scraped into harvest buffer [50 mmol/L Tris (pH 7.5), 150 mmol/L NaCl, 2.5 mmol/L EDTA, 1 mmol/L sodium vanadate, 1% NP40, 10 μg/mL aprotinin, 10 μg/mL leupeptin, 0.25 mg/mL AEBSF]. The cell suspension was passed through a 22-gauge needle several times. Nuclear debris and unbroken cells were then removed by centrifugation at $10,000 \times g$ for 10 minutes. The protein concentration was measured using the BCA Protein Assay (Pierce, Rockford, IL). Equal amounts of protein were separated by SDS-PAGE, transferred to Immobilon-P membranes, and blotted with antibodies according to the manufacturer's recommendations. Antibody complexes were visualized by chemiluminescent detection using ECL reagent.

**Immunofluorescence analysis.** Cells used in immunofluorescence analysis were seeded onto two-well chamber slides (Nalge Nunc International, Rochester, NY) or eight-well chamber slides (Falcon, Bedford, MA) coated with poly-L-lysine and allowed to adhere to the slide (16 hours) before they were fixed with 4% paraformaldehyde. Following washing in PBS and treatment with 0.2% Triton X-100, the cells were blocked with 10% normal goat serum in PBS for 30 minutes at room temperature and then incubated with the indicated antibodies in PBS for 1 hour at room temperature or 4°C overnight. Following washing, visualization was achieved by incubation with species-specific secondary antibodies for 1 hour at room temperature. Alexa Fluor 488/568–conjugated anti-rabbit and anti-mouse antibodies were used to detect polyclonal and monoclonal primary antibodies, respectively. Following further washing in PBS, nuclei were stained with 4′,6-diamidino-2-phenyl-indole (4 μg/mL in PBS) for 5 minutes at room temperature. Cells were washed in PBS, mounted, and then visualized with a Leica (Exton, PA) SP/NT spectral confocal microscope.

Quantification of the findings was based on a minimum of three independent experiments (range, 3-8) for each study. In each experiment, multiple, random, nonoverlapping fields were counted without the observer's knowledge of the treatment or sample. Within each field, all cells were included, except in transfection experiments where only transfected cells (as identified by markers: HA, GFP, or Cy3) were counted. For each condition, a minimum of 100 cells was evaluated (range, 104-1,336; average, ∼250). Differences between experimental groups were compared using paired Student's $t$ tests.

**Drug treatment.** Inhibitors (20 and 200 nmol/L rapamycin, 10 μmol/L LY294002, 1 μmol/L wortmannin, 50 μmol/L PD98059, 40 mmol/L lithium chloride, and 50 μg/mL cycloheximide) were added to 10% FBS-DMEM/F-12 and incubated for 1, 5, 12, or 24 hours. After treatment, cells were fixed and incubated with antibodies as described previously for analysis by indirect immunofluorescence. In parallel experiments, cells were lysed in harvest buffer and equal amounts of protein were analyzed for phospho-S6 expression by Western blotting as described above. To determine whether rapamycin can change caveolin-1 localization after nocodazole treatment, $Tsc2-/-$ cells were treated with 40 μmol/L nocodazole for 1 hour followed with treatment of 200 nmol/L rapamycin for 5 hours.

**Microtubule-binding assay.** After starving for 16 hours, cells were rinsed with PEM (80 mmol/L PIPES, 1 mmol/L MgCl$_2$, 1 mmol/L EGTA) and swelled for 5 minutes with EM (2 mmol/L EGTA, 1 mmol/L MgCl$_2$). Cells were lysed in PEM lysis buffer (PEM plus 1 mmol/L DTT and protein inhibitors) by Dounce homogenization. The cell lysates were cleared by centrifugation at $100,000 \times g$ (TLA 55 rotor) for 1 hour at 4°C and concentrated by Amicon Ultra-4 10,000 MWCO (Millipore). Samples (120 μg total protein) were incubated in the presence or absence of Taxol-stabilized tubulin (Cytoskeleton, Denver, CO) in PEM with 5 mmol/L MgCl$_2$ and 20 μmol/L Taxol and incubated for 15 minutes at 37°C. To separate the microtubules, samples were layered onto 10% sucrose cushion in PEM containing 20 μmol/L Taxol and spun at $100,000 \times g$ (TLS 55 rotor) at 20°C for 40 minutes. The microtubule-containing pellets were rinsed once in PEM, separated by SDS-PAGE, and analyzed by Western blot and Coomassie blue stain.

**Time-lapsed video microscopy.** Following transfection of GFP-EB1 or GFP-tubulin construct for 48 hours, cells were imaged with Nikon (Melville, NY) inverted Diaphot 200 microscope coupled to Princeton Instruments MicroMax CCD camera and filter wheels for integrated operation via MetaMorph software (Princeton Imaging, West Chester, PA). Movies were edited with MetaMorph software. Data analyses and interpretation were from raw images acquired once every 2 to 5 seconds and monitored for 2 to 4 minutes.

## Results

**Effects of mTOR inhibitors on protein transport.** Based on the observations that membrane proteins, such as caveolin-1, are mislocalized in cells devoid of TSC1 or TSC2 (21), we tested the hypothesis that aberrant protein transport is a consequence of mTOR activation. First, we examined the effects of down-regulating mTOR by rapamycin on caveolin-1 distribution in these cells. Caveolin-1 is a structural protein of caveolae, which normally localizes to specialized microdomains of the plasma membrane known as lipid rafts, but in $Tsc2-/-$ (EEF-8) REFs most of the caveolin-1 resided in punctate cytoplasmic vesicles (Fig. 1*A, top row, left*) as described previously (21). Exposure of these cells to rapamycin at 20 nmol/L did not significantly alter the caveolin-1 localization (Fig. 1*A*). However, when treated at 10-fold higher concentration (200 nmol/L) for 24 hours (but not 1 hour), rapamycin was able to induce a redistribution of cytoplasmic caveolin-1 to the plasma membrane (Fig. 1*A*). In dose-response and time-course experiments, we found that >100 nmol/L rapamycin for a minimum of 5 hours was required to see an effect on protein localization (data not shown). Given that 20 nmol/L rapamycin effectively inhibits mTOR activity on p70S6K and ribosomal S6 (Fig. 1*B*), these results show that the effects of rapamycin on protein localization did not correlate with its biochemical activity on mTORC1. To confirm these observations, a second independently derived $Tsc2-/-$ cell line (EEF-4A) from the Eker rat (data not shown) and a $Tsc1-/-$ MEF cell line (Fig. 1*A, bottom row*) were tested under identical conditions, and the results showed the same effects on caveolin-1 localization. Treatment of wild-type cells ($Tsc2+/+$ REF and $Tsc1+/+$ MEF) with 20 or 200 nmol/L rapamycin (24 hours) did not alter the distribution of caveolin-1 (Supplementary Fig. S1). These data suggest that the abnormal intracellular trafficking of caveolin-1 in $Tsc$-null cells can be rescued by rapamycin but is unlikely to be mediated by the mTORC1 complex.

To further analyze the contribution of mTOR activity on caveolin-1 transport in the mutant cells, they were treated with the mTOR kinase inhibitors, wortmannin and LY294002. Although wortmannin (1 μmol/L) blocked ribosomal S6 phosphorylation in $Tsc2-/-$ cells, it failed to significantly change caveolin-1 distribution, thus confirming that the rapamycin-induced shift in caveolin-1 localization is independent of p70S6K activity (Fig. 1*B*; Supplementary Fig. S2). However, prolonged exposure (12 hours) to LY294002

(10 μmol/L) rescued the abnormal caveolin-1 localization in *Tsc1*- and *Tsc2*-null cells to the same extent as rapamycin (200 nmol/L; Fig. 1*B*; Supplementary Fig. S2). Further, the inhibition of mitogen-activated protein kinase with PD98059, GSK3 with lithium chloride, and protein synthesis with cycloheximide in the mutant cells did not change caveolin-1 distribution, suggesting a specific effect of mTOR on protein localization (Fig. 1*B*). Collectively, these results are consistent with the hypothesis that mTOR activity plays a role in
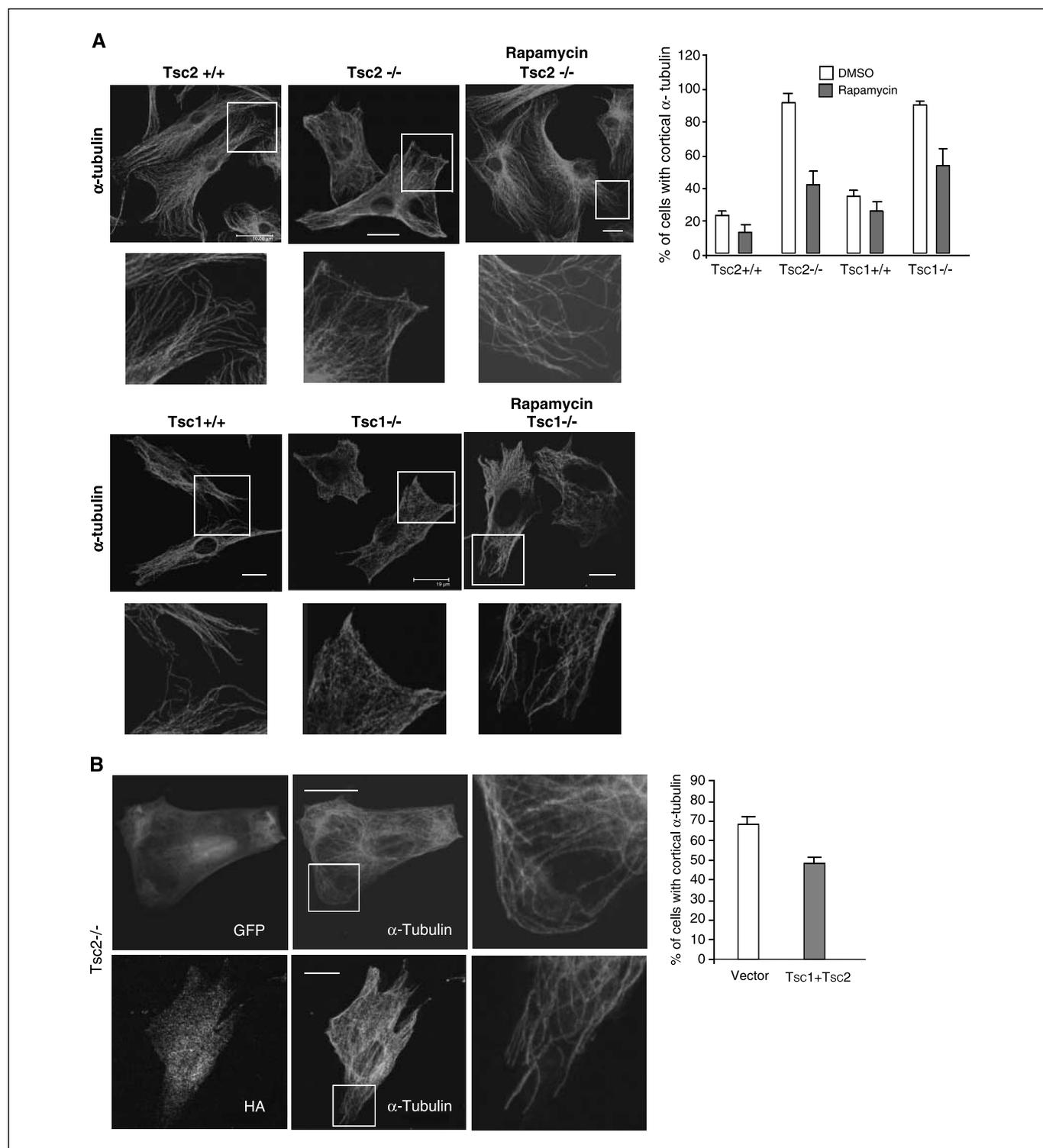


**Figure 3.** Effects of the mTOR pathway on microtubules. *A,* microtubule organization of *Tsc2*+/+ and *Tsc2*−/− cells (*top*) and *Tsc1*+/+ and *Tsc1*−/− cells (*bottom*) is illustrated by immunofluorescence staining for α-tubulin. *Bottom row,* enlarged images of the boxed areas. *Right,* effects of rapamycin (200 nmol/L, 24 hours) on microtubules. Bar, 20 μm. *Columns,* quantitation of the results. *B, Tsc2*−/− cells were cotransfected with myc-Tsc1 and HA-Tsc2 or GFP control vector. Transfected cells were analyzed with dual immunofluorescence staining for HA (shown) or myc (not shown) and α-tubulin. *Columns,* percentage of cells with thick cortical pattern of α-tubulin.

caveolin-1 transport in *Tsc*-null cells and that the lack of effect of wortmannin could be explained by the short half-life of the inhibitor.

**Modulation of caveolin-1 localization by components of the mTOR pathway.** We have shown previously that exogenously expressed Tsc1 and Tsc2 in *Tsc2−/−* cells were sufficient to relocalize cytoplasmic caveolin-1 to the plasma membrane (21). Next, we studied the effects of downstream effectors of TSC1/TSC2 on protein localization. In mammalian cells, mTOR is activated by Rheb whose activity is negatively regulated by the GAP activity of TSC2. mLST8 is an essential component of the mTORC1 and mTORC2 complexes, and the expression of both Rheb and mLST8 have been shown to up-regulate mTOR activity, thus simulating the loss of TSC1/TSC2 (7, 8, 24). To test the effects of up-regulating mTOR on caveolin-1 localization, we used an isogenic line of *Tsc2+/+* REFs in transient transfection of Rheb and mLST8 expression vectors followed by dual immunofluorescence analyses for caveolin-1 and exogenous-tagged proteins (HA and myc). Figure 2*A* shows that Rheb expression in these fibroblasts promoted redistribution of plasma membrane caveolin-1 to the cytoplasm coincident with an increase in mTOR activity as illustrated by elevated phospho-S6 levels. Note that nontransfected or vector-transfected cells showed prominent plasma membrane staining of caveolin-1 (Fig. 2*A*). The mean proportion of *Tsc2+/+* cells with predominant cytosolic caveolin-1 increased from 25% to 52% and 73% following wild-type and constitutively active Rheb(Q64L) expression, respectively. Similarly, overexpression of myc-mLST8, but not the vector control, significantly increased the number of cells with cytosolic caveolin-1

staining and was associated with increased p70S6K and S6 phosphorylation (Fig. 2*B*). Thus, up-regulation of mTOR activity in wild-type cells is sufficient to inhibit caveolin-1 plasma membrane localization.

Based on our observations using chemical inhibitors (see Fig. 1), the effects of mTOR on protein trafficking did not correlate with p70S6K activity. p70S6K acts downstream of the mTORC1 complex (mTOR/raptor/mLST8) that controls ribosome biogenesis and protein translation. To directly address the influence of p70S6K on caveolin-1 localization, cells were transfected with p70S6K expression constructs whose activities were confirmed by immunoblot analysis of phospho-S6 (data not shown). As shown in Fig. 2*C*, there was no significant change in caveolin-1 distribution in either *Tsc2+/+* or *Tsc2−/−* cells expressing wild-type p70S6K compared with vector control. Further, expression of an inactive kinase mutant, p70S6K(K123R), in *Tsc2−/−* cells failed to restore caveolin-1 to the plasma membrane. However, introduction of an inactive kinase mutant of mTOR (S2035T/D2357E) significantly reduced the proportion of *Tsc2−/−* cells with predominant cytoplasmic caveolin-1 (Fig. 2*C*). This confirms that caveolin-1 localization is sensitive to the direct manipulation of mTOR but not dependent on p70S6K activity.

Because mTOR exists in a second complex, mTORC2 (mTOR/rictor/mLST8), which is resistant to the acute effects of rapamycin, our observations linking chronic, high-dose rapamycin exposure to caveolin-1 transport suggest the possible involvement of mTORC2. It has been proposed that prolonged treatment with rapamycin can potentially down-regulate mTORC2 through the sequestration of



**Figure 3** *Continued.* *C, Tsc2+/+* cells were transfected with myc-tagged mLST8 or Rheb(Q64L) and analyzed with anti-myc and anti-α-tubulin antibodies in dual immunofluorescence analysis. Control cells were transfected with GFP-expressing vector. Bar, 20 μm. *Columns,* percentage of cells with thick cortical pattern of α-tubulin.
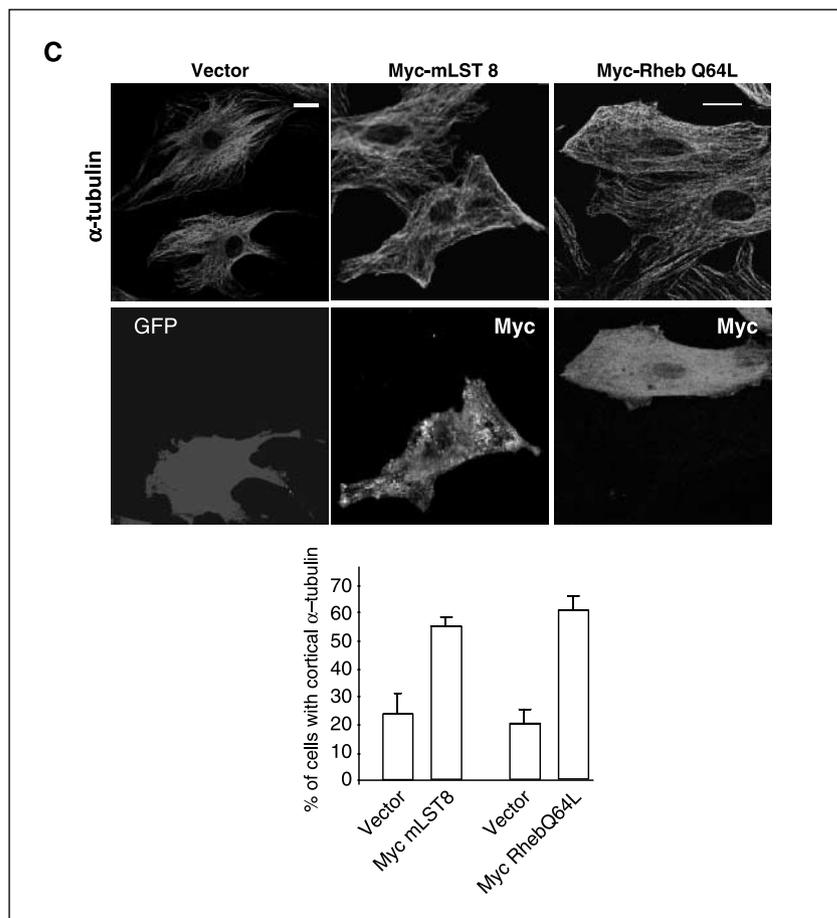
intracellular mTOR molecules by the rapamycin/FKBP12 complex (25). Indeed, Fig. 2*D* shows that chronic (24-hour) treatment with rapamycin at 200 nmol/L in *Tsc2*−/− REFs resulted in significant suppression of AKT (Ser$^{473}$) phosphorylation, a mTORC2-specific site (25). Neither a 1-hour treatment at 200 nmol/L nor a 24-hour treatment at 20 nmol/L was sufficient to suppress Ser$^{473}$ phosphorylation. Of note, AKT activity is reduced in *Tsc2*−/− cells due to the negative feedback effects by constitutively activated p70S6K in these cells (26). Down-regulation of p70S6K by rapamycin released this inhibition resulting in AKT activation in the mutant cells. Importantly, whereas the relative levels of AKT (Ser$^{473}$) phosphorylation increased with time in *Tsc2*−/− cells exposed to low-dose rapamycin, the opposite was true with high-dose treatment, suggesting that mTORC2 is down-regulated only with prolonged, high-dose rapamycin. These findings correlate with the effects of rapamycin on caveolin-1 localization and are consistent with the possible involvement of mTORC2 in regulating caveolin-1 transport.

**Effects of mTOR activity on microtubule arrangements.** Microtubules are known to play a role in intracellular trafficking of proteins and vesicles (reviewed in ref. 27). Specifically, post-Golgi caveolin-1 transport is dependent on microtubule integrity, such that the depolymerization of microtubules with nocodazole abolished the rapamycin-induced redistribution of caveolin-1 to the plasma membrane in *Tsc2*−/− cells (Supplementary Fig. S3). To determine the mechanism by which mTOR influences protein transport, we investigated the effects of mTOR activity on microtubule organization. To visualize microtubules in wild-type and mutant cells, immunofluorescence analysis using α-tubulin antibody was done. *Tsc2*+/+ and *Tsc1*+/+ cells exhibited thin strands of α-tubulin fibers that extend radially toward the periphery of the cells (Fig. 3*A, left*). In comparison, cells lacking Tsc2 or Tsc1 showed significant blunting of the peripheral strands associated with a prominent α-tubulin "band" around the perimeter of the cells (Fig. 3*A, middle*). This appearance suggests bundling of cortical tubulin along the edges of protruding lamellae. The same abnormal phenotype was found in a second, independent *Tsc2*−/− REF line (EEF-4A; data not shown). The average percentages of these cells displaying the prominent cortical microtubules were 91% in *Tsc2*−/− (EEF-8) and 90% in *Tsc1*−/− compared with 23% in *Tsc2*+/+ and 35% in *Tsc1*+/+ cells (*P* < 0.05, between mutant and wild-type cells; Fig. 3*A*). Intriguingly, treatment with rapamycin (200 nmol/L, 5 hours) resulted in a significant reduction in the proportion of *Tsc1*−/− and *Tsc2*−/− cells with prominent cortical microtubules (54% and 42%, respectively) and an appearance similar to that of the wild-type cells (Fig. 3*A, right*). Short-term exposure (i.e., <5 hours) or low-dose rapamycin (i.e., <200 nmol/L) did not have an effect on microtubule organization (data not shown) consistent with the observations on caveolin-1 distribution shown in Fig. 1*A*.

To confirm the influence of the TSC/mTOR pathway on microtubule organization, we examined the effects of Tsc1/Tsc2 in *Tsc2*−/− cells and, conversely, mLST8 and Rheb(Q64L) in *Tsc2*+/+ cells. Introduction of exogenous wild-type Tsc1/Tsc2 in the mutant cells partially rescued the abnormal microtubule phenotype (Fig. 3*B*), whereas overexpression of Rheb and mLST8 in wild-type cells promoted the formation of prominent α-tubulin-positive bundles around the cell periphery similar to those seen in *Tsc2*−/− cells (Fig. 3*C*). These observations strongly suggest that mTOR activity exerts an influence on microtubule organization.

Next, to characterize the nature of the microtubule disorganization in *Tsc2*−/− cells, we immunostained these cells with antibodies specific for acetylated form of tubulin, which represents the stabilized pool. Figure 4*A* illustrates a difference in acetylated tubulin distribution at the cortical regions of the cells, confirming that there is an abnormal accumulation of stabilized microtubules around the periphery of the mutant cells. This may be due to perturbation of microtubule dynamics and/or organization. To examine this, we analyzed the growth of microtubule toward the cell periphery in live cells using EB1 as a marker for microtubule plus-ends. On transient transfection of GFP-tagged EB1 in wild-type cells, an orderly progression of fluorescent signals located at the tips of microtubules was seen migrating radially toward the cell edge (Fig. 4*B, top*; Supplementary Movie S1). The movement of these EB1-associated microtubule complexes was largely unidirectional, and as they approached the cell perimeter, the plus-end signals underwent pause, shortening (catastrophes), and regrowth (rescues) as described previously (28). At the cell margins, the EB1 signals disappeared as they lost their association with the microtubule tips. In comparison, GFP-EB1 expression in *Tsc2*−/− cells displayed a significantly different pattern of movement. In addition to the radial tracking, EB1 "comets" were seen moving parallel to the cell cortex in multiple directions and not infrequently in opposing orientations (Fig. 4*B, bottom*; Supplementary Movie S2). These microtubule trajectories are best appreciated by tracing the tracks of individual EB1 signals over time as shown in the accompanying vector diagrams (Fig. 4*B, far right*). In *Tsc2*−/− cells, many EB1 signals were found to track along the cell perimeter rather than projecting perpendicular to it. Nonetheless, the plus-end microtubules in *Tsc2*−/− cells did undergo pause and catastrophes at various random points along the cell periphery. These observations suggest that the defect seen in *Tsc2*−/− cells is predominantly due to a disruption in microtubule organization rather than dynamics.

One possible explanation for the abnormal cortical microtubule trajectories in the mutant cells may be due to the failure of the radial microtubules to halt their growth as they approach the cell cortex (e.g., missensing of cortical signals). Instead, these microtubules may continue to extend by bending their trajectories as they approach the periphery to become parallel to the plasma membrane. To test this hypothesis, we examined the pattern of newly formed microtubules in cells expressing GFP-tubulin. Forty-eight hours post-transfection, analyses of live cells showed distinct patterns of microtubule growth as illustrated in Fig. 4*C*. Although the majority of microtubules stopped growing once they reached the subcortical region in wild-type cells, the GFP-tubulin signals in *Tsc2*−/− cells clearly showed continued growth around the cell periphery resulting in subcortical accumulation of microtubules. These observations confirm the results of our immunofluorescence studies and provide a plausible explanation for the abnormal microtubule phenotype.

**Down-regulation of CLIP-170 rescues abnormal caveolin-1 transport and microtubule organization.** How does mTOR affect microtubule organization? A link between them has been suggested previously to involve the microtubule plus-end binding protein, CLIP-170/restin (29). It has been shown that mTOR directly binds and phosphorylates CLIP-170 at rapamycin-sensitive sites to positively regulate its association with microtubules (30). However, the mTOR-dependent phosphorylation sites have not been mapped, so the direct effect of mTOR on CLIP-170 function is not well understood. Besides microtubules, CLIP-170 also interacts with

**Figure 4.** Microtubule disorganization in *Tsc2*−/− cells. *A,* immunofluorescence analysis of acetylated tubulin in *Tsc2*+/+ and *Tsc2*−/− cells. *Bottom,* enlarged images of the boxed areas. *B,* plus-end tracking of GFP-EB1 in transiently transfected *Tsc2*+/+ and *Tsc2*−/− cells. *Arrows,* examples of plus-end movements at the indicated time intervals. *Right,* vector diagrams of accumulative paths and directions of individual GFP signals captured over 2 minutes. For complete videos of time-lapsed analyses, see Supplementary Movies S1 and S2. *C,* analysis of newly synthesized microtubules in *Tsc2*+/+ and *Tsc2*−/− cells transiently expressing GFP-tubulin. Note the extensive bending and curvilinear projections associated with the accumulation of microtubules in the subcortical zone of the *Tsc2*−/− cells.
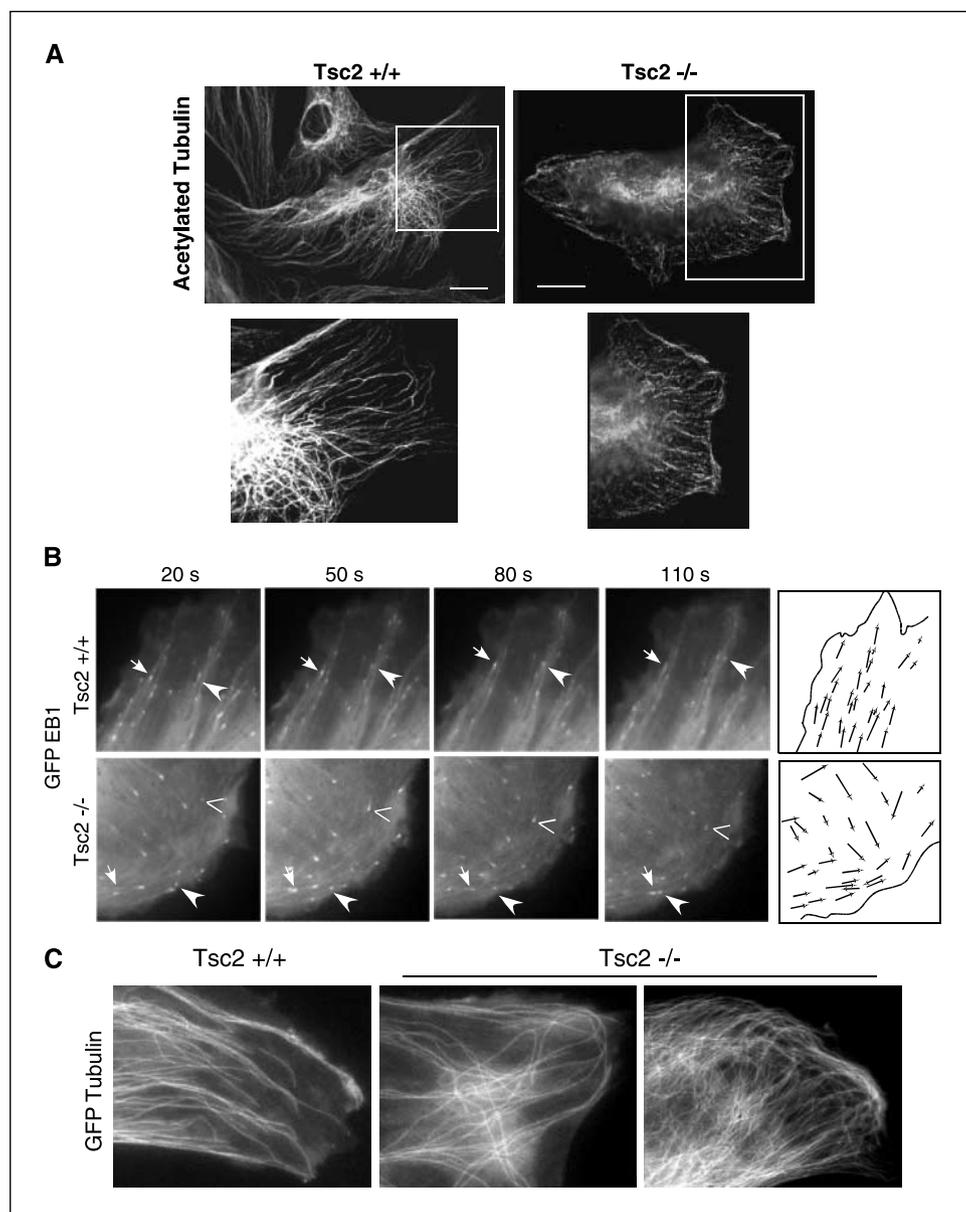
proteins that are involved in vesicular transport and is purported to play a role in the assembly and docking of vesicles to microtubules along which cargo is transported (reviewed in ref. 31). Given our finding that mTOR regulates the microtubule cytoskeleton, we speculated that the increased mTOR activity in *Tsc2*−/− cells might result in abnormal CLIP-170-microtubule function, thus giving rise to microtubule disorganization and protein mislocalization.

To compare the relative amounts of microtubules bound to CLIP-170 in the two cell types, we did *in vitro* microtubule-binding assays using Taxol-stabilized microtubules as substrate. Figure 5*A* shows that in the absence of TSC2 the amount of CLIP-170 that coprecipitated with exogenous microtubules in the pellet (*lane 4*) was greater than that of the wild-type cells (*lane 2*, relative intensities to microtubules: 1.76 for −/− versus 1.52 for +/+). This is consistent with the findings in yeast as reported by Musch (27). To further address the function of CLIP-170 in protein transport and microtubule function in *Tsc2*−/− cells, we examined the effects

of down-regulating CLIP-170 on caveolin-1 distribution using small interference RNA (siRNA). Compared with the negative control, Cy3-luciferase siRNA, transfection of siRNA directed toward the rat CLIP-170 gene resulted in a significant reduction in its expression in both *Tsc2*+/+ and *Tsc2*−/− cells (Fig. 5*B*). Of note, the transfection efficiency was higher in *Tsc2*+/+ cells, which may account for a more complete reduction in the expression of CLIP-170. Figure 5*C* shows that caveolin-1 was relocated from the cytoplasm to the plasma membrane in *Tsc2*−/− cells transfected with Cy3-tagged CLIP-170 siRNA but not with control siRNA. The percentage of *Tsc2*−/− cells exhibiting plasma membrane caveolin-1 increased from 25% with control siRNA to 62% with CLIP-170 siRNA. Concurrent with the effects on caveolin-1 localization, reduction in CLIP-170 expression in *Tsc2*−/− cells also restored the microtubule architecture (Fig. 5*D*). In contrast to the thick cortical microtubule bands in cells transfected with control siRNA, those with Cy3-labeled CLIP-170 siRNA showed finer, peripheral α-tubulin strands similar to that of the wild-type cells.

The proportion of *Tsc2*−/− cells with thick cortical α-tubulin decreased from 90% to 31% following transfection of CLIP-170 siRNA. Down-regulation of CLIP-170 in wild-type cells did not significantly changed caveolin-1 distribution or microtubule organization.

To further show the influence of mTOR/CLIP-170 on microtubule organization, we analyzed +TIP tracking using GFP-EB1 in mutant cells pretreated with rapamycin or trans-fected with Cy3-labeled CLIP-170 siRNA. As shown in Fig. 6*A* and Supplementary Movie S3, the chaotic trajectories of microtubule growth observed in *Tsc2*−/− cells were "normal-ized" by the down-regulation of either mTOR with rapamycin or CLIP-170 by siRNA. Vector diagrams of these cells show a return to orderly radial projections of microtubules resembling the *Tsc2*+/+ phenotype (see Fig. 4*B* for comparison). Together, these
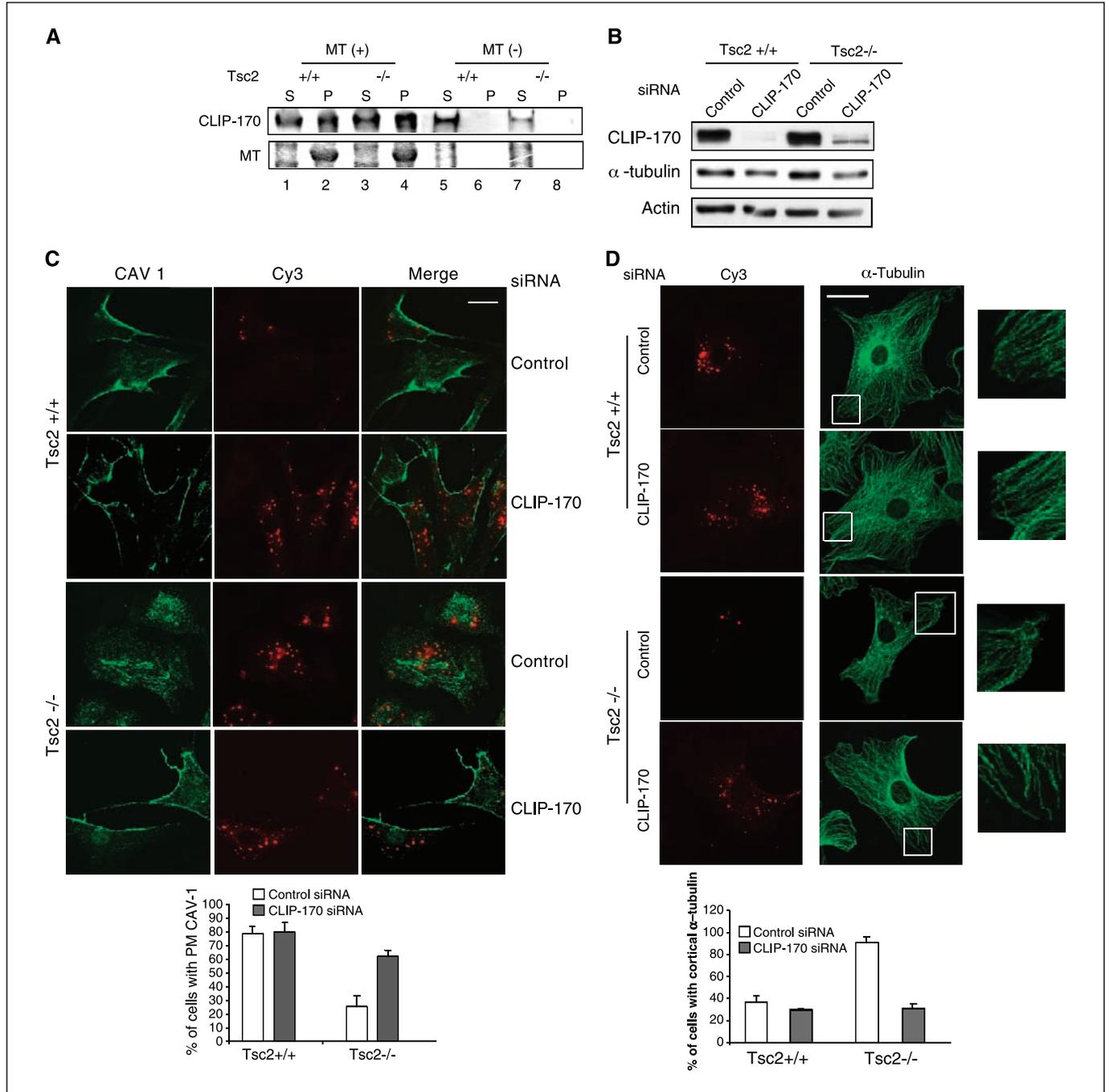


**Figure 5.** Effects of CLIP-170 on caveolin-1 localization and microtubule arrangement. *A, in vitro* microtubule-binding assay. Cell lysates were incubated with Taxol-treated tubulin and centrifuged at $100,000 \times g$ for 40 minutes. Supernatant (*S*) and microtubule-containing pellet (*P*) were analyzed for CLIP-170 by Western blotting. Microtubule (*MT*) was detected by Coomassie blue staining. Samples without tubulin (-) served as controls. *B,* cells were transfected with indicated siRNA and harvested after 48 hours. Western blot analyses of CLIP-170, α-tubulin, and actin. *C,* immunofluorescence analysis of caveolin-1 following transfection with CLIP-170 or control Cy3-conjugated siRNA in *Tsc2*+/+ and *Tsc2*−/− cells. *Columns,* percentages of cells with plasma membrane caveolin-1. *D,* microtubule organization was examined by immunofluorescence analysis of α-tubulin in *Tsc2*+/+ and *Tsc2*−/− cells following siRNA transfection. *Right,* detailed microtubule morphology in these cells. *Columns,* percentages of cells with prominent cortical α-tubulin.

**Figure 6.** Influence of mTOR/CLIP-170 on microtubule organization. *A, Tsc2−/−* cells were transiently transfected with GFP-EB1 construct and control (*top two*) or CLIP-170 (*bottom row*) siRNA. One set of control siRNA cells (*middle row*) was exposed to rapamycin (200 nmol/L) for 12 hours before time-lapsed videomicroscopy. Selected images at 20, 40, 70, and 80 seconds. *Right,* vector diagrams of paths of GFP-positive signals of the respective cells photographed over 2 minutes at 1 frame/2 seconds. For complete videos, see Supplementary Movie S3. *B,* model of TSC2/mTOR-mediated protein transport. CLIP-170 serves as a putative effector of mTOR to regulate microtubule organization and transport.
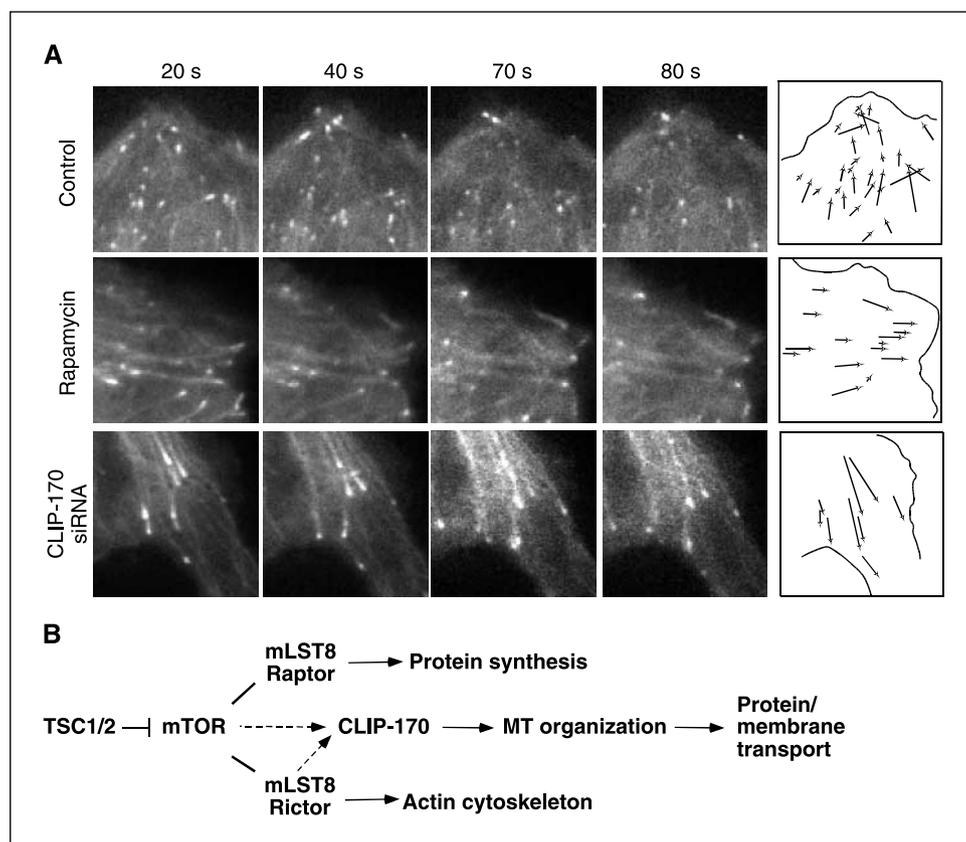
data strongly support a role of CLIP-170 in protein transport *in vivo* and suggest that it may act downstream of TSC2/mTOR to regulate microtubule organization.

## Discussion

In the present study, we uncovered a novel functional relationship between microtubule-dependent protein trafficking and mTOR. Previous studies have reported that cells deficient in TSC2 are defective in protein transport (20, 21). Kleymenova et al. identified a loss of polycystin-1 at the plasma membrane of *Tsc2*-deficient cells due to its sequestration in the Golgi apparatus (20). We subsequently showed that post-Golgi transport of VSVG is significantly delayed in *Tsc2−/−* cells resulting in its apparent mislocalization (21). These observations suggest a more general defect in the transport of proteins that are destined for the plasma membrane. In both loss-of-function and gain-of-function experiments, we showed in this study that the transport of caveolin-1 is under the influence of mTOR in mammalian cells. We attribute this to a function of mTOR in regulating the microtubule cytoskeleton that plays a critical role in membrane trafficking. Both *Tsc1*- and *Tsc2*-null cells possess abnormal organization of the subcortical microtubule network that can be rescued by down-regulating mTOR or its effector, CLIP-170, and in doing so restore a normal pattern of caveolin-1 distribution. Further, our data provide direct evidence that CLIP-170 is involved in microtubule-dependent membrane trafficking perhaps through its effects on sensing cortical signals necessary for establishment and/or maintenance of peripheral microtubule organization.

The mTOR pathway has been associated with multiple functions that connect environmental cues to cellular responses in growth, proliferation, and differentiation (reviewed in ref. 32). The best characterized of these functions is its role in regulating protein synthesis and cell growth via the downstream effectors p70S6K and 4E-BP1 that are phosphorylated by the rapamycin-sensitive mTORC1 complex (14, 15). However, less is known about the mechanism of sensing the environment for nutrient and energy sources in mammalian cells. One possibility suggested by our data is that mTOR regulates protein/vesicular trafficking through its influence on microtubule organization (Fig. 6*B*). This is supported by earlier observations showing that the trafficking of 4F2hc amino acid transporter to the plasma membrane in mammalian cells was disrupted in the presence of a kinase-inactive mTOR (33). Accordingly, plasma membrane localization of nutrient transporters could be under the control of mTOR. Further studies are needed to address the role of the mTOR pathway in regulating microtubule-dependent nutrient uptake.

Our findings suggest that mTOR-regulated transport is not mediated by mTORC1 because the effects of rapamycin on protein transport were observed at concentrations (e.g., 200 nmol/L) that were significantly higher and durations (e.g., >5 hours) that were much longer than are necessary for mTORC1 inhibition. Further, the modulation of the mTORC1 target, p70S6K, did not affect protein localization. This is consistent with the observations by Choi et al. showing sensitivity of various microtubule functions to rapamycin at concentrations similar to that used in this study (29). Conversely, Edinger et al. reported an apparent lack of effect of low-dose (e.g., 20 nmol/L) rapamycin on amino acid transporter localization in FL5.12 cells (33). Hence, we propose that

the alteration in protein trafficking in cells exposed to high concentrations of rapamycin may be indirectly due to the sequestration of mTOR via the rapamycin-FKBP12 complex, thus leading to reduced activity of the TORC2 (mTOR/rictor/mLST8) complex as suggested previously (16, 17). Our observation that protracted high-dose rapamycin exposure reduced AKT (Ser$^{473}$) phosphorylation is consistent with this hypothesis. Alternatively, there may exist a yet undefined mTOR complex that affects transport, which is partially sensitive to rapamycin. Future analyses of the role of rictor in this setting will provide direct insights into the contribution of mTORC2 to protein trafficking.

The mechanism by which mTOR affects protein transport is at least partially attributed to its effect on microtubule organization. The dramatic differences in α-tubulin immunofluorescence of the *Tsc1*- and *Tsc2*-null cells along with the results of tubulin-GFP and GFP-EB1 videomicroscopy in live cells point to a defect of microtubule plus-ends to sense cortical signals. We further showed that a putative mTOR effector, CLIP-170, plays a role in microtubule-dependent trafficking. The link between TOR signaling and CLIP-170 was initially highlighted by the identification of a mutant of the yeast homologue, Bik1, which was hypersensitive to rapamycin (29). Bik1p is required for microtubule function during mitosis and mating through its interaction with microtubule and kinesin motor proteins (34). An analogous role of its mammalian homologue, CLIP-170/restin, has been proposed in the regulation of membrane transport and cell polarity (reviewed in refs. 31, 35, 36). Because TOR can phosphorylate CLIP-170 at rapamycin-sensitive sites (30), we propose a model whereby the function of CLIP-170 is altered in the setting of constitutive mTOR activation. The detectable increase of CLIP-170-microtubule binding in *Tsc2*−/− cells is consistent with previous evidence showing a positive regulation of the microtubule-binding behavior of CLIP-170 (30). Thus, the persistent CLIP-170 interaction with microtubules in the mutant cells could interfere with the ability of the microtubule plus-ends to sense cortical sites, tether to actin, and/or form capping structures. To further analyze the effects of mTOR on CLIP-170 function, we await the identification of the putative rapamycin-sensitive phosphorylation sites. This notwithstanding, we showed that down-regulation of CLIP-170 by siRNA was sufficient to rescue the plasma membrane localization of caveolin-1 and to reverse the cortical microtubule arrangement toward a wild-type phenotype.

Functional links between microtubules and activated cortical sites have been proposed. Among them, CLIP-170 has been shown to interact with the actin-binding protein, IQGAP1, on activation of Rac1/Cdc42 activity (37, 38). During cell polarization, Rac1/Cdc42 activated sites serve to capture microtubules to cortical regions resulting in proper microtubule alignment. Future studies will address the influence of mTOR on CLIP-170-IQGAP interaction and actin-microtubule association at the cell cortex. Other proteins, such as ACF7, APC, and PKCζ, are also relevant to microtubule dynamics and guidance. In particular, it is interesting to note the similarity in cortical microtubule disorganization of the ACF7-null cells compared with that of the *Tsc2*−/− cells; both display skewed microtubule trajectories (28). ACF7 has been characterized as an integrator of microtubule-actin dynamics by binding to both during cell polarization (28). Its presence at the leading edge seems to be essential to the maintenance of the cytoskeleton network during cell migration. It remains to be determined if ACF7 plays a role downstream of TSC2 in the regulation of microtubule organization and how the function of other proteins that are involved in plus-end tracking may be affected by the mTOR pathway.

In summary, this study highlights a novel function of mTOR in its regulation of microtubule organization. Protein transport and membrane trafficking are microtubule-dependent activities that are perturbed when mTOR is constitutively activated. Our study suggests that CLIP-170 may serve as an effector of mTOR in regulating the microtubule network and provides further evidence that CLIP-170 plays a role in membrane trafficking. The effects of mTOR on microtubules in mammalian cells may have implications in nutrient exchange, cell signaling, polarity, and division, all of which are relevant to the pathogenesis of human cancers.

## Acknowledgments

## References

1. Vignot S, Faivre S, Aguirre D, Raymond E. mTOR-targeted therapy of cancer with rapamycin derivatives. Ann Oncol 2005;16:525–37.
2. Inoki K, Corradetti MN, Guan KL. Dysregulation of the TSC-mTOR pathway in human disease. Nat Genet 2005;37:19–24.
3. Li Y, Corradetti MN, Inoki K, Guan KL. TSC2: filling the GAP in the mTOR signaling pathway. Trends Biochem Sci 2004;29:32–8.
4. Stocker H, Radimerski T, Schindelholz B, et al. Rheb is an essential regulator of S6K in controlling cell growth in *Drosophila*. Nat Cell Biol 2003;5:559–65.
5. Saucedo LJ, Gao X, Chiarelli DA, Li L, Pan D, Edgar BA. Rheb promotes cell growth as a component of the insulin/TOR signalling network. Nat Cell Biol 2003;5:566–71.
6. Zhang Y, Gao X, Saucedo LJ, Ru B, Edgar BA, Pan D. Rheb is a direct target of the tuberous sclerosis tumour suppressor proteins. Nat Cell Biol 2003;5:578–81.
7. Inoki K, Li Y, Xu T, Guan KL. Rheb GTPase is a direct target of TSC2 GAP activity and regulates mTOR signaling. Genes Dev 2003;17:1829–34.
8. Castro AF, Rebhun JF, Clark GJ, Quilliam LA. Rheb binds tuberous sclerosis complex 2 (TSC2) and promotes S6 kinase activation in a rapamycin- and farnesylation-dependent manner. J Biol Chem 2003;278:32493–6.
9. Potter CJ, Pedraza LG, Xu T. Akt regulates growth by directly phosphorylating Tsc2. Nat Cell Biol 2002;4:658–65.
10. Inoki K, Li Y, Zhu T, Wu J, Guan KL. TSC2 is phosphorylated and inhibited by Akt and suppresses mTOR signalling. Nat Cell Biol 2002;4:648–57.
11. Dan HC, Sun M, Yang L, et al. Phosphatidylinositol 3-kinase/Akt pathway regulates tuberous sclerosis tumor suppressor complex by phosphorylation of tuberin. J Biol Chem 2002;277:35364–70.
12. Inoki K, Zhu T, Guan KL. TSC2 mediates cellular energy response to control cell growth and survival. Cell 2003;115:577–90.
13. Shaw RJ, Bardeesy N, Manning BD, et al. The LKB1 tumor suppressor negatively regulates mTOR signaling. Cancer Cell 2004;6:91–9.
14. Hara K, Maruki Y, Long X, et al. Raptor, a binding partner of target of rapamycin (TOR), mediates TOR action. Cell 2002;110:177–89.
15. Kim DH, Sarbassov DD, Ali SM, et al. mTOR interacts with raptor to form a nutrient-sensitive complex that signals to the cell growth machinery. Cell 2002;110:163–75.
16. Sarbassov dos D, Ali SM, Kim DH, et al. Rictor, a novel binding partner of mTOR, defines a rapamycin-insensitive and raptor-independent pathway that regulates the cytoskeleton. Curr Biol 2004;14:1296–302.
17. Jacinto E, Loewith R, Schmidt A, et al. Mammalian TOR complex 2 controls the actin cytoskeleton and is rapamycin insensitive. Nat Cell Biol 2004;6:1122–8.

18. Wullschleger S, Loewith R, Hall MN. TOR signaling in growth and metabolism. Cell 2006;124:471–84.

19. Roberg KJ, Bickel S, Rowley N, Kaiser CA. Control of amino acid permease sorting in the late secretory pathway of *Saccharomyces cerevisiae* by SEC13, LST4, LST7 and LST8. Genetics 1997;147:1569–84.

20. Kleymenova E, Ibraghimov-Beskrovnaya O, Kugoh H, et al. Tuberin-dependent membrane localization of polycystin-1: a functional link between polycystic kidney disease and the TSC2 tumor suppressor gene. Mol Cell 2001;7:823–32.

21. Jones KA, Jiang X, Yamamoto Y, Yeung RS. Tuberin is a component of lipid rafts and mediates caveolin-1 localization: role of TSC2 in post-Golgi transport. Exp Cell Res 2004;295:512–24.

22. Loewith R, Jacinto E, Wullschleger S, et al. Two TOR complexes, only one of which is rapamycin sensitive, have distinct roles in cell growth control. Mol Cell 2002; 10:457–68.

23. Fang Y, Vilella-Bach M, Bachmann R, Flanigan A, Chen J. Phosphatidic acid-mediated mitogenic activation of mTOR signaling. Science 2001;294:1942–5.

24. Kim DH, Sarbassov dos D, Ali SM, et al. GβL, a positive regulator of the rapamycin-sensitive pathway required for the nutrient-sensitive interaction between raptor and mTOR. Mol Cell 2003;11:895–904.

25. Sarbassov dos D, Guertin DA, Ali SM, Sabatini DM. Phosphorylation and regulation of Akt/PKB by the rictor-mTOR complex. Science 2005;307:1098–101.

26. Harrington LS, Findlay GM, Gray A, et al. The TSC1-2 tumor suppressor controls insulin-PI3K signaling via regulation of IRS proteins. J Cell Biol 2004; 166:213–23.

27. Musch A. Microtubule organization and function in epithelial cells. Traffic 2004;5:1–9.

28. Kodama A, Karakesisoglou I, Wong E, Vaezi A, Fuchs E. ACF7: an essential integrator of microtubule dynamics. Cell 2003;115:343–54.

29. Choi JH, Adames NR, Chan TF, Zeng C, Cooper JA, Zheng XF. TOR signaling regulates microtubule structure and function. Curr Biol 2000;10:861–4.

30. Choi JH, Bertram PG, Drenan R, Carvalho J, Zhou HH, Zheng XF. The FKBP12-rapamycin-associated protein (FRAP) is a CLIP-170 kinase. EMBO Rep 2002;3:988–94.

31. Rickard JE, Kreis TE. CLIPs for organelle-microtubule interactions. Trends Cell Biol 1996;6:178–83.

32. Harris TE, Lawrence JC, Jr. TOR signaling. Sci STKE 2003;2003:re15.

33. Edinger AL, Linardic CM, Chiang GG, Thompson CB, Abraham RT. Differential effects of rapamycin on mammalian target of rapamycin signaling functions in mammalian cells. Cancer Res 2003;63: 8451–60.

34. Berlin V, Styles CA, Fink GR. BIK1, a protein required for microtubule function during mating and mitosis in *Saccharomyces cerevisiae*, colocalizes with tubulin. J Cell Biol 1990;111:2573–86.

35. Carvalho P, Tirnauer JS, Pellman D. Surfing on microtubule ends. Trends Cell Biol 2003;13: 229–37.

36. Akhmanova A, Hoogenraad CC, Drabek K, et al. Clasps are CLIP-115 and -170 associating proteins involved in the regional regulation of microtubule dynamics in motile fibroblasts. Cell 2001;104: 923–35.

37. Fukata M, Watanabe T, Noritake J, et al. Rac1 and Cdc42 capture microtubules through IQGAP1 and CLIP-170. Cell 2002;109:873–85.

38. Watanabe T, Wang S, Noritake J, et al. Interaction with IQGAP1 links APC to Rac1, Cdc42, and actin filaments during cell polarization and migration. Dev Cell 2004;7:871–83.

**AACR** American Association for Cancer Research

# Regulation of Microtubule-Dependent Protein Transport by the TSC2/Mammalian Target of Rapamycin Pathway

Xiuyun Jiang and Raymond S. Yeung

| | |
|---|---|
| **Updated version** | Access the most recent version of this article at:<br>http://cancerres.aacrjournals.org/content/66/10/5258 |
| **Supplementary Material** | Access the most recent supplemental material at:<br>http://cancerres.aacrjournals.org/content/suppl/2006/05/17/66.10.5258.DC1 |

| | |
|---|---|
| **Cited articles** | This article cites 38 articles, 11 of which you can access for free at:<br>http://cancerres.aacrjournals.org/content/66/10/5258.full#ref-list-1 |
| **Citing articles** | This article has been cited by 3 HighWire-hosted articles. Access the articles at:<br>http://cancerres.aacrjournals.org/content/66/10/5258.full#related-urls |

| | |
|---|---|
| **E-mail alerts** | Sign up to receive free email-alerts related to this article or journal. |
| **Reprints and Subscriptions** | To order reprints of this article or to subscribe to the journal, contact the AACR Publications Department at pubs@aacr.org. |
| **Permissions** | To request permission to re-use all or part of this article, use this link<br>http://cancerres.aacrjournals.org/content/66/10/5258.<br>Click on "Request Permissions" which will take you to the Copyright Clearance Center's (CCC)<br>Rightslink site. |